

## **Electrochemical behaviour of metal-supported SOFCs under high fuel utilization and their durability**

I. Antepara\*, L. Diaz, M. Rivas, L. Otaegi, N. Gomez, I. Villarreal, A. Laresgoiti

Ikerlan- Energía, Parque Tecnológico de Álava, Juan de La Cierva,1 E-01510  
Miñano, Álava, Spain

\*corresponding author:

I. Antepara\*, Ikerlan- Energía, Parque Tecnológico de Álava, 01510 Miñano, Spain  
tel.: +34 945 297032, fax: +34 945 296926, e-mail: [inigoantepara@hotmail.com](mailto:inigoantepara@hotmail.com)

### **ABSTRACT**

The aim of this project was to study whether the oxidation resistance of cells is affected while working under high fuel utilization. A previous study measured the weak oxidation resistance for very porous samples (measured porosity ~ 70%) in H<sub>2</sub> with high H<sub>2</sub>O content (over 50%) in the interval from 600°C to 800°C. Thus, additional tests were carried out with cells.

Crofer22APU-supported SOFCs were produced by scalable cost competitive routes. One of the highly-porous cells (calculated porosity 45%) was run under

high fuel utilization conditions (calculated fuel utilization 56%), and a further two in H<sub>2</sub>-50%H<sub>2</sub>O. Another cell, with low porosity (calculated porosity 20%), was kept working in the same H<sub>2</sub>-50%H<sub>2</sub>O atmosphere for many hours.

Durability tests with cells of different porosities confirmed that this is the main variable concerning degradation issues while working under high fuel utilization.

**KEYWORDS:** Solid Oxide Fuel Cells, durability and damage tolerance, Utilization, Modeling

**ABBREVIATIONS:** FU, fuel utilization; HSW, hot sanitary water; FSS, ferritic stainless steel; VPS, vacuum plasma spraying; ASR, area specific resistance; CFD, computational fluid dynamics; EIS, electrochemical impedance spectroscopy; OCP, open circuit potential; SEM, scanning electron microscope; EDS, energy dispersive X-ray analysis; DBL, diffusion barrier layer.

## 1 INTRODUCTION

Many domestic appliances run on fuel gases such as natural gas or propane. It is always desirable to convert the energy contained in the fuel gas into electricity (high-grade energy) rather than into heat (low-grade energy). High electricity conversions can be obtained using fuel cells, as their theoretical electrical efficiency is very high. Yet it is obvious that high fuel utilization (FU) is essential; if the fuel gas supplied is not converted, electrical efficiency cannot be high. Eventually, the energy consumed by auxiliaries must be reduced to a minimum.

Based on these assumptions, the prototype of a domestic generator that produces HSW and electricity will be built as a result of Ikerlan's SOFC project [1]. An operating temperature of below 800°C is also desirable, so that certain expensive ceramic components, like the support, can be replaced with metal components. Ikerlan's approach is similar to other research units [2], although it has planned a tubular geometry instead of a planar one for the prototype. High power density is not needed in domestic applications, thus, tubular cells were the option because they can be sealed more easily and lower stresses result from thermal cycles.

Prior work was carried out to study the influence of different aspects of the SOFC anode environment on the oxidation behaviour of porous samples made of Crofer22APU [3]. Although low oxygen activity can protect the alloy from the catastrophic oxidation behaviour observed at higher oxygen activities, this is not compatible with a cell working at high FU, when SOFCs produce high amounts of vapour that are thermodynamically in equilibrium with relatively high oxygen partial pressures ( $pO_2$ ). It will therefore be a problem of kinetics in the real cell; with certain positive effects reducing the oxidizing process and other negative effects accelerating it. Open porosity (and surface area) is the main variable influencing the oxidation of porous samples.

Other research groups have reached similar conclusions [2]; 0.04 m<sup>2</sup>/g was proposed as the maximum specific surface area for porous Crofer22APU to resist 5000 hours at 800°C.

The data for Ni metal-supported cells working at a FU of 50% is also available in the literature. A stack did not degrade for the initial 2100 hours [4].

However, there are fewer references in the literature for a metal-supported SOFC made of ferritic stainless steel (FSS) under high FU. One test has been reported for a cell in hydrogen containing 50% water vapour at 600°C. The porosity of the support was lower than 20%, and the composition was ANSI-430 (Fe-17Cr) or SUS-447J (Fe-30Cr-2Mo) (not specified in the article). Although no degradation measurements were presented, the cell worked steadily for at least 1400 hours [5]. Problems involving the oxidation of the FSS support are more readily found in the literature. At Forschungszentrum Jülich a CroFer22APU metal-supported 16 cm<sup>2</sup> cell was fed with 1 l/min of hydrogen-3% water vapour and 1 l/min of air at a current density of 0.3 A/cm<sup>2</sup> for 190 hours at 800°C. Catastrophic oxidation was observed [6]. From these data, a water vapour content of 6% at the outlet can be calculated. This low water vapour content does not cause catastrophic oxidation after 190 hours at 800°C, so this oxidation could be better explained if its cause can be attributed to the sealing. In addition, M. Brandner observed catastrophic oxidation in cells working at 800°C and 0.3 A/cm<sup>2</sup> after 165 hours [2], although in this case it is not possible to calculate the water vapour content at the outlet. In the end, higher diffusion overpotentials were measured for these cells, indicating that fuel gas supply was more difficult, as the open porosity of the metal support became blocked. Small particle size is required for VPS deposition, which increases surface area and leads to oxidation. Chromia is formed under a deposited ceramic layer, increasing ASR.

Ohmic resistance increased in the case of a Plansee IT11 metal-supported solid oxide electrolyzer cell (SOEC) when a gas mix of H<sub>2</sub>-43%H<sub>2</sub>O was electrolyzed at

800°C. After 2000 hours the metal support (H<sub>2</sub> electrode, working as a SOFC it will be the anode) was oxidized [7].

At Ikerlan, no substantial oxidation was observed in a cell with a CroFer22APU metallic substrate after 1000 hours at 300 mA/cm<sup>2</sup> and 800°C. Experiments were run under low FU, and water vapour concentration was always below 5% at the outlet [8].

The aim of the following tests is to study the electrochemical behaviour and durability of CroFer22APU metal-supported SOFCs with different porosities under high FU. CFD modelling of these experiments was used to obtain profiles of temperature and concentration of the main species (H<sub>2</sub> and H<sub>2</sub>O), in order to fully understand the processes.

## **2 EXPERIMENTAL**

Powder CroFer22APU metal tubes were consolidated at high temperature in hydrogen until enough mechanical properties were obtained (70% porosity). Ceria barrier layer was deposited to prevent Cr, Fe and Ni interdiffusion between the support and anode layer. A thin YSZ electrolyte was deposited by dip-coating and then co-fired in a non-oxidising atmosphere at 1350°C. LSF cathode was subsequently dip-coated and fired in situ prior to electrochemical characterisation. Tubes of 5 cm length and an active area of 4 cm<sup>2</sup> were systematically produced. Pt paste and mesh were used on the cathode side as current collector. The cell and gas manifolds were mounted in an alumina tube. Ceramic paste from Aremco Products Inc. (Ultra-temp 516) was used as sealing material for durability testing.

The tests were performed using a red-y gas flow controller (GSC-A9SA-EE21 from Vögtlin Instruments AG, 300-10 mln/min). The controller had to work at its lowest flow (the largest error possible), so it was calibrated using a soap film flow meter (0101-0113, 1-10-100 mL, Hewlett-Packard). Pure H<sub>2</sub> was forced to bubble into the humidification system (HS-AWF from FuelCellStore.com). This system was fed with water from a purifier (AP-3 model from Puragua Systems). The flow at the outlet of the humidification system was supposed to be saturated, so controlling the temperature of the water rendered it possible to control the H<sub>2</sub>/H<sub>2</sub>O ratio. The final humidity at the outlet of the humidification system was measured with a humidity and temperature transmitter (Vaisala HMT337). The whole pipe from this point to the inlet on the alumina tube was heated to over 100°C to avoid condensation.

Field-Point commercial modules based on a voltage and current generation system and LabWindows/CVI software (National Instruments, NI) were used. Current-voltage (I-V) measurements were performed at 800 °C at an increasing current rate of 10 mA/min. Durability tests were carried out at constant current density, but trying to maintain the potential between 0.8-0.7 V, and recording data over time.

The microstructure was examined in a FEI 200 Quanta FEG scanning electron microscope (SEM) and with energy dispersive X-ray analysis (EDS).

Electrochemical Impedance Spectroscopy (EIS) measurements were performed using a Solartron 1266 Frequency Response Analyser coupled to a 1286 Electrochemical Interface. The impedance spectra were recorded under an applied current corresponding to cell performance at 0.7 V with a 10 mV AC signal amplitude over the 106 to 0.01 Hz frequency range. ASR, ohmic resistance (R<sub>o</sub>)

and the polarization resistance ( $R_p$ ) contributed by the electrodes (normally the cathode) were calculated from EIS data [9].

Samples with controlled porosity were prepared to study their resistance against oxidation. Long tubes were consolidated and samples of 1cm height were cut. Then, they were sintered at high temperature in hydrogen until the porosity of these porous substrates was around 45%.

### **3 CFD MODELING**

Simulations were performed with commercial CFD code Fluent v. 6.3.26 (double precision solver), in a 580.000 cell quad mesh. The geometry consists of a symmetrical portion of 30°. Fluent has a special SOFC model for determining cell electrochemistry. Flow was assumed to be laminar and incompressible, until a steady-state solution was reached.

Total current was imposed as a boundary condition, to obtain the voltage at the electrodes, chemical species and temperature distributions throughout the domain, as well as the current density distribution at the electrolyte.

#### **3.1 Model equations**

“Standard” RANS for incompressible flow, as provided in Fluent code [10], were used for the simulations, including Species Transport Model, with full multicomponent diffusion, thermal diffusion and diffusion energy source.

SOFC Model provided by Fluent includes the calculation of electric potential (Nernst potential, ohmic losses in the electrolyte, and activation losses at the electrode-electrolyte interfaces), current density at the electrolyte, current

conduction in conductive regions, heat sources due to electrochemical reactions, activation overpotential and ohmic losses.

The main parameters for the SOFC Model are as follows:

- The conductivities used can be found in table 1. The conductivities from data from the supplier were considered for Crofer22APU and Pt paste. Measurements were taken at Ikerlan for the anode and cathode.
- No contact resistances were taken into account between the different cell layers (Pt mesh over a tubular cell tends to tighten).
- Exchange current densities ( $j_{0a} = 1000 \text{ A/m}^2$  for the anode and  $j_{0c} = 100 \text{ A/m}^2$  for the cathode) are the parameters with the strongest influence on cell voltage. Both have been chosen as the most appropriate for the system being modelled, according to a previous CFD-based Design of Experiment study.

### 3.2 Boundary Conditions

The boundary conditions are summarized as follows:

- Anode, cathode and its current collector paste, and support solid zones are defined as porous zones with a porosity of 30%, a tortuosity of 3, and a permeability of  $10^{13} \text{ 1/m}^2$  in every direction. Tortuosity is based on literature review [11]. Porosity is an average for the two cells used in our experimental work. Experimental data was used to extrapolate the permeability.



- Mass and energy source terms due to electrochemical reactions are defined by the SOFC model at the anode and the cathode. Energy source terms due to Joule heating are defined for all the conductive materials.
- Pt wires are used as current collectors.
- The gas, as in a real case, enters the domain through an alumina tube inside the cell. This gas composition at the anode inlet is  $H_2$ -3% $H_2O$  mass flow (table 2), the same as in the first experiment (4.1 paragraph).
- The cell in the experiment is inside an oven at 800°C. Thus, air at 800°C is allowed to flow outside the cathode. Air mass flow in table 2, used as the boundary condition for mass flow, is estimated from another CFD calculation with Fluent, modelling the buoyancy-driven air flow inside an oven at 800°C.
- Total current (table 2) is imposed as the boundary condition at the electrolyte.

### 3.3 Solution procedure

The solution procedure was as follows [10]:

- For the initial solution: 0 m/s for velocity, 100%  $N_2$  gas composition, 800°C for temperature, 0.8 V for the cell potential on the cathode side (0 V otherwise).
- About 100 iterations are performed with the energy source term on the electrolyte surface only. Volumetric energy source terms are then enabled.
- The solution is considered to be converged when the residuals are down to  $10^{-6}$ , except for energy to  $10^{-7}$  and cell potential to  $10^{-8}$ .

- A pressure-based, implicit solver is used and the solution is first-order accurate in all the equations.

## 4 RESULTS

Adequate sintering shrinkage is one of the main issues regarding the quality of metal-supported SOFCs produced by cosintering [12]. Past experience at Ikerlan shows that when sintering shrinkage is not between 15-20% the electrolyte has cracks or they form more easily, and open circuit potential (OCP) is usually lower than 1 V or zero. However, adequate sintering shrinkage is not enough; at Ikerlan cells with good shrinkage gave no OCP, sometimes due to bad sealing, sometimes due to possible cracks. Thus, OCP is a good indicator of the quality of both the cell and subsequent gas-tightness. OCPs as high as 1.11 V were obtained for one cell at the laboratory (non-commercial interconnects) - almost the maximum theoretically attainable at 800°C with air and H<sub>2</sub>-3%H<sub>2</sub>O. The maximum OCP in the literature, an OCP of 1.1 V was reported at DLR [13].

### 4.1 Cell at high FU

One cell with 4 cm<sup>2</sup> of active area was selected for this test. The shrinkage after sintering was slightly low, but OCP (1.07 V) and the electrochemical data (420 mW/cm<sup>2</sup> @ 0.7 V) were very good. The final porosity of the metal substrate was calculated (initial porosity 70% and shrinkage) to be 45%.

It is possible to calculate the surface area of the support of the cell through the Konezy-Carman equation [14]:

$$S = k \cdot \left[ \frac{1 - P^3}{\alpha (1 - P)^2} \right]^{\frac{1}{2}}$$

where  $P$  is porosity  
 $\alpha$  is dynamic viscosity  
 $S$  is surface area  
and  $k$  is a constant

But, apart from the porosity  $P$ , the dynamic viscosity  $\alpha$  is also needed. Using the correlation of J. Bukowiecki [15] (constant particle size):

$$\alpha = k' \cdot P$$

where  $k'$  is a constant

The following relationship between surface area and porosity is obtained:

$$S = k'' \frac{P}{1 - P}$$

where  $k''$  is a constant

It was possible to complete the relationship, fitting the data from Hg porosimetry:

$$S = 0.081 \frac{P}{1 - P} + 0.00583$$

where  $S$  is in  $\text{m}^2/\text{g}$ .

The surface area of this cell was calculated through this equation;  $0.072 \text{ m}^2/\text{g}$ . This value was used to predict the lifetime of the support with data from [2]; a lifetime between 200 and 400 hours.

### Electrochemical behaviour

1) Measurements while reducing  $\text{H}_2$  flow for high FU

Figure 1 shows I-V curves measured with H<sub>2</sub> flows at 800°C starting from 150 down to 10 mln/min (maximum error of the gas flow controller was +-4.5ml/min, so a soap film flow meter was used for calibrating). OCP at low flow was lower (the quality of the cell and gas-tightness have even more influence when gas flows are reduced for high FU tests). In order to study whether hysteresis has any influence on the electrochemical behaviour of the cell, the H<sub>2</sub> flow was increased to 150 mln/min and then lowered to 10 mln/min. Repeatability was good at both working points.

Data from EIS is shown in table 3. R<sub>o</sub> is constant in all the measurements (~ 0.2 Ωcm<sup>2</sup>), but R<sub>p</sub> increases with smaller flows (from 0.16 to 0.27 Ωcm<sup>2</sup>). This is due to diffusion problems when small flows are used. A slower current rise rate for the I-V measurements is needed with low flows. As the H<sub>2</sub> flow steadily decreases, fuel utilization (in this case H<sub>2</sub> converted to H<sub>2</sub>O) increases at high current densities and this considerably changes the composition of the anode atmosphere. This major change in the composition influences the cell's electrochemical response until equilibrium is reached. It thus takes longer to reach a stable response.

## 2) Durability test at high FU

The durability test started at a working point of 0.8 V and 200 mA/cm<sup>2</sup>, as can be seen in figure 2. The cell was fed with a humidified H<sub>2</sub> flow of 10mln/min (3% water content), which is a calculated fuel utilization of 56% (between 40% and 100% taking into account the controller error, but calibration showed that the error was very small). After 2 hours the voltage of the cell was well below 0.8 V. Current density was therefore lowered to 150mA/cm<sup>2</sup> (calculated FU, 43%) with the same

H<sub>2</sub> flow. The voltage dropped continuously, but after 25 hours it fell to zero (the lowest limit of the I-V measuring equipment). This value is lower than the predicted lifetime. The water vapour content of the exhaust gases at the outlet was not measured.

#### Microstructure after durability test

Figure 3 shows the SEM image of a cross-section of the cell working at 800°C at high FU. The type of oxidation is catastrophic, but not uniform. Two things are worth mentioning; it is located near the anode, and not along the whole anode but under the area covered by the cathode, namely, the electrochemically active area.

Previous work on the oxidation behaviour of porous samples made of Crofer22APU does not help to explain this kind of oxidation. From that study the main two variables (all the tests with a temperature inside the oven of 800°C) were: water vapour content and sample porosity. Current density is another variable, but its influence is not so important. If no uniform oxidation was expected, higher oxidation at the outlet would be expected, as the water vapour content is higher. This did not happen, as similar oxidation is observed from the inlet to the outlet.

Two more cells with adequate sintering shrinkages and porosities of around 50% were tested in H<sub>2</sub>-50%H<sub>2</sub>O. The same type of oxidation was recorded after a few hours.

#### 4.2 Oxidation of samples with a porosity of 50%

The resistance against oxidation of samples with a porosity of 50% (slightly over the 45% of the porosity of the porous substrate of the cell from the FU test) was studied in H<sub>2</sub>-50%H<sub>2</sub>O at 850°C for 100h.

Figure 4 shows the SEM image of the sample. The sample is severely oxidized, but not as much as the case of the electrochemically active area of the substrate of the cell in paragraph 4.1.

#### 4.3 Cell working in H<sub>2</sub>-50%H<sub>2</sub>O atmosphere

Another cell with 4 cm<sup>2</sup> of active area was produced for this test. The aim was to study the influence of porosity. It was not possible to obtain a cell with a porosity of around 20% with the ceramic diffusion barrier layer (DBL), so no such layer was introduced.

Using the same relationship between surface area and porosity, the calculated surface area of the support of this cell is 0.024 m<sup>2</sup>/g. The predicted lifetime is over 100.000 hour, which means that reducing the surface area by a factor of 3, the predicted lifetime is multiplied by 50. The reason for such a long predicted lifetime is the equation in [2]. Comparing both cells, the lifetime prediction for this second cell is:

$$t_B = (100 - 400h) \cdot 3^{\frac{1}{n}}$$

where the exponential coefficient  $n$  is between 0.2 and 0.4 [2]

#### Electrochemical behaviour

##### 1) Measurements while changing the anode atmosphere

Data from the electrochemical measurement (175 mW/cm<sup>2</sup> @ 0.7 V) were not as good as in the first case. The R<sub>o</sub> is more than double (Table4) because of the anode's lower Ni content. The R<sub>p</sub> with H<sub>2</sub>-3%H<sub>2</sub>O was 0.26 Ωcm<sup>2</sup>, higher than in the previous case. The reason: worse transport of H<sub>2</sub> to the anode due to a lower

porosity, and/or worse electrochemical activity of the anode due to a lower Ni content.

Smaller flows than the former ones were needed for a high FU test, but this was not possible with the red-y gas flow controller. Thus, in order to have an atmosphere thermodynamically similar to the previous case (same %H<sub>2</sub>O), an atmosphere of 200 mln/min with a water vapour content of 50% was produced with the humidification system. When increasing the water vapour content of the anode atmosphere to 50%, OCP decreased, as is to be expected theoretically, and the OCP obtained was again almost the maximum attainable. R<sub>p</sub> increased slightly to 0.33 Ωcm<sup>2</sup>.

## 2) Durability test at high FU

After this last measurement in H<sub>2</sub>-50%H<sub>2</sub>O, the cell was maintained at a constant current density of 100 mA/cm<sup>2</sup> for 150 hours. This current density corresponded to a voltage of 0.8 V, but as can be seen in figure 5 the measured voltage is not very stable. For 150 hours, R<sub>o</sub> improved down to 0.4 Ωcm<sup>2</sup>, and R<sub>p</sub> was more or less constant, indicating that the restriction to H<sub>2</sub> diffusion did not increase.

### Microstructure after durability test

Figure 6 is a SEM image of a cross-section of the cell working at 800°C in H<sub>2</sub>-50%H<sub>2</sub>O. No important oxidation was observed: neither uniform nor located in a specific area.

#### 4.4 CFD modelling

As a way to explain the anomalous oxidation of the first cell (working temp. 800°C, fuel H<sub>2</sub>-3% H<sub>2</sub>O), a CFD simulation was carried out. Conclusions from this model cannot be extrapolated to longer cells, stacks, etc.

A profile of the cell H<sub>2</sub>O mole fraction can be found in figure 7. H<sub>2</sub> with 3% H<sub>2</sub>O is coloured in blue, and exhaust H<sub>2</sub> (56% H<sub>2</sub>O) in red. Gas flowing inside the small tube inside the cell increases its H<sub>2</sub>O content because of both the high diffusion of H<sub>2</sub>O in H<sub>2</sub>, and the low flows used in the high FU test, although it is a non-electrochemically active zone of the cell. The H<sub>2</sub>O returns to the inlet and the atmosphere composition from the inlet to the outlet is fairly uniform. Thus, the entire active part of the cell is working under the same atmosphere composition. What's more, it is the highest H<sub>2</sub>O content possible.

The cell temperature profile is also available in figure 8. The model calculates a 15°C increase in the temperature of the electrochemically active part of the cell, due to H<sub>2</sub> reacting with oxygen ions (even although contact resistances between layers are zero).

## 5 CONCLUSIONS

OCP is a good indicator of the quality of both the cell and subsequent gas-tightness. High OCPs were obtained, almost always the maximum attainable, except when feeding the cell with low flows of H<sub>2</sub>. The influence of a small leak is greater in the case of low flows, as compared to high flows of H<sub>2</sub>.



The electrochemical response of the cell fed with a low flow of  $H_2$  is slower, with some kind of inertia when trying to attain stable EIS data under these conditions. Nevertheless, I-V curves were measured with a high  $H_2$  flow, then with a low flow and, finally, with a high flow again. No hysteresis was measured, the cell seemed unaffected by working under low flows, and good repeatability was attained.

Unlike low porosity cells with no Ce DBL, those with high porosity recorded oxidation near the anode after durability testing in atmospheres with high water vapour contents (from the humidification system or by-product of the reaction on the anode side), and not along the whole anode, but instead under the area covered by the cathode - the electrochemically active area.

High diffusion of  $H_2O$  in  $H_2$  was inferred from the CFD model of the cell working at high FU, also because of the low flows that have to be used in this high FU test. The  $H_2O$  produced returns to the inlet due to the short length of the cell. Thus, the entire active part of the cell was working under the same atmosphere composition, the highest possible. This result cannot be extrapolated to longer cells. Furthermore, a small increase of  $15^\circ C$  in the temperature of the electrochemically active part of the cell was deduced. As in the case of  $H_2$  diffusion, this temperature increase cannot be extrapolated to longer cells. The temperature profile of a longer cell cannot be compared to this, as the interconnect needs to be changed, different types of cooling configurations can be implemented (cross-flow, parallel-flow or counter-flow), etc. Nevertheless, the conditions at the outlet of a long cell can be similar to these.

It was possible to calculate a lifetime for the support through the porosity. But the predicted lifetimes can be considered as maximum. Real lifetimes of the cells are shortened because of accelerated oxidation around the electrochemically active zone of the cell.

The main variables of the anode atmosphere, namely, temperature and water vapour content, were similar when testing low and high porosity cells. Thus, porosity, one of the most important variables concerning the oxidation of porous Crofer22APU samples [3], was the main responsible for the different oxidation resistance observed. But the oxidation of the support near the electrochemically active area is faster than predicted. Thus, some extra aspects accelerate the oxidation process in this zone.

A way of retarding this catastrophic oxidation is to adjust the porosity of the metal support, trying to find an optimum between the minimum possible surface area and an adequate H<sub>2</sub> diffusion to the anode. Changing the composition may also help; FSS with higher %Cr content, like ITM (Plansee), may retard the Cr depletion of the metallic substrate. Pure Ni was used successfully without cycling [4]. The tubular geometry of our system may temper the differences between the coefficients of thermal expansion of Ni and ceramic components, although the Ni resistance to redox cycles is lower. Finally, there is no great difference in the final oxidation state in the 600°C to 800°C range [3], although the kinetics are lower at 600°C.

## 6 FUTURE WORK

More tests are planned to find an explanation for the acceleration of the oxidation process of the support near the electrochemically active area. Although it is under study, the proposed mechanisms for this oxidation of the cell are:

a) Ni diffusion from the anode to the metallic support. If so, the oxidation could be clearer observed in the cell with no DBL, but the DBL is not a perfect barrier and the Ni content in the cell with DBL is higher. The diffusion of Ni inside the metallic support can convert the ferritic phase of the support into austenitic one. The proposed mechanism in [16] is that higher thermal expansion coefficient of the austenitic phase causes stresses.

b) The negative effect of the current flow was studied in [3], although it is small.

c) The temperature increases near the electrochemically active area in the CFD model because of  $H_2$  reacting with  $O_2$ , as no contact resistance is taken into account. It is a low temperature increase, but the  $H_2$  atmosphere with more than 50%  $H_2O$  oxidizes Crofer22APU at 800°C [3]. And each small temperature increase therefore causes even more oxidation. When the support in contact with the anode starts oxidizing, ASR increases due to the high resistivity of the oxides. When oxides appeared in the interface between anode and support, the contact resistance of this interlayer increased, as well as the temperature; higher ASR and the control maintaining the current density constant caused higher ohmic losses. Higher temperature around the electrochemically active zone of the cell, accelerated oxidation, higher ASR... even higher temperature. The oxidation process accelerated because of the control maintaining the current density

constant. In a real stack when controlling the potential, the current density will decay when the ASR starts increasing, the temperature will not increase, and a slower oxidation process is expected.

d) On a relatively porous support it is not easy to built-up a thin electrolyte layer, although one of the cells with a porosity of 50% reached an OCP of 1.11V (indicating the good quality of the electrolyte). But some pores or cracks (and electrolyte leakages) would become bigger near the electrochemically active area because of thermal stresses there, and therefore H<sub>2</sub> in the anode would react with air from the cathode. In this case, Ni would be the first oxidized metal.

## **ACKNOWLEDGEMENTS**

This work has been possible thanks to the ETORTEK (GENEDIS) and SAIOTEK projects of the Basque Government as well as to the Mondragon Group, Fagor and Mondragon Componentes.

In memory of my cousin Oscar and my father.

## **REFERENCES**

- [1] I. Villarreal, C. Jacobson, A. Leming, Y. Matus, S. Visco, L. De Jonghe, *Electrochem. Solid-State Lett.* 6 (2003) A178-A179S.
- [2] M. Brandner, *Herstellung einer Metall/Keramik Verbundstruktur fuer Hochtemperaturbrennstoffzellen in mobilen Anwendungen.* PhD thesis JUEL-4238, Research Center Juelich, Juelich, Germany, 2006.

- [3] I. Antepará, M. Rivas, I. Villarreal, N. Burgos, F. Castro, ASME Journal of Fuel Cell Science and Technology 7 (2010) 061010.
- [4] S. Takenoiri, N. Kadokawa, K. Koseki, Journal of Thermal Spray Technology 9 (2000) 360-363.
- [5] N. Oishi, Y. Yoo, SOFC-XI (2009) 739-744.
- [6] D. Hathiramani, R. Vaßen, J. Mertens, D. Sebold, V.A.C. Haanappel, D. Stöver, Ceramic Engineering and Science Proceedings, Cocoa Beach, FL, 2006, pp. 55-65.
- [7] G. Schiller, A. Ansar, M. Lang, O. Patz, Journal of Applied Electrochemistry 39 (2009) 293-301.
- [8] L.M. Rodríguez-Martínez, L. Otaegi, M. Rivas, N. Gómez, M. Álvarez, A. Zabala, N. Arizmendiarieta, I. Antepará, I. Villarreal, A. Laresgoiti, ECS Meeting Abstracts 902 (2009) 1578-1578
- [9] K.R. Cooper, M. Smith, Journal of Power Sources 160 (2006) 1088-1095.
- [10] Fluent User's Manual
- [11] R. Campana, A. Larrea, R.I. Merino, I. Villarreal, V.M. Orera, Boletín de la Sociedad Española de Cerámica y Vidrio, 47 (4) (2008) 189-195
- [12] J.D. Carter, T.A. Cruse, J.M. Ralph, D.J. Myer, Powder metallurgy and solid oxide fuel cells, Int. Conf. On Powder Metallurgy & Particulate Materials, Las Vegas, 2003.
- [13] A. Ansar, Z. İlhan, J. Arnold, Plasma Sprayed Metal Supported SOFCs having Enhanced Performance and Durability, Proc. of the Int. Thermal Spray Conf., Las Vegas, 2009.

- [14] R.M. German, Powder Metallurgy Science, Second Edition, MPIF, Princeton, NJ, 1994
- [15] G. Hoffman, D. Kapoor, Int J Powder Metall Powder Technol, 12(4) (1976) 281-296.
- [16] S.T. Ertl, Untersuchungen zur oxidationsbedingten Lebensdauer von Chromstählen für die Anwendung in der Hochtemperaturbrennstoffzelle (SOFC), Ph.D. Thesis RWTH Aachen, Fakultät für Maschinenwesen, 2006.

## FIGURE CAPTIONS

Fig 1. I-V performance of a tubular metal-supported cell tested under different H<sub>2</sub> flows.

Fig 2. Degradation curves for a tubular metal-supported SOFC tested at 800°C under high FU.

Fig 3. SEM image of a cross section of the cell working at 800°C at high FU.

Fig 4. SEM image of a cross section of the porous sample oxidized at 850°C in H<sub>2</sub>-50%H<sub>2</sub>O.

Fig 5. Voltage curve for a tubular metal-supported SOFC tested at 800°C in H<sub>2</sub>-50%H<sub>2</sub>O at a constant current density of 100 mA/cm<sup>2</sup>.

Fig 6. SEM image of a cross section of the cell working at 800°C in H<sub>2</sub>-50%H<sub>2</sub>O.

Fig 7. FLUENT model of a cell, oven temperature 800°C and fuel H<sub>2</sub>-3%H<sub>2</sub>O. Contours of mole fraction of H<sub>2</sub>O.

Fig 8. FLUENT model of a cell, oven temperature 800°C and fuel H<sub>2</sub>-3%H<sub>2</sub>O. Contours of temperature.

## **TABLES**

Table 1. Summary of properties for the porous layers.

Table 2. Data for the portion modelled. For the whole cell, multiply the figures by 6.

Table 3. Ohmic resistance ( $R_o$ ) and polarization resistance ( $R_p$ ) data for the cell at high and low  $H_2$ -3% $H_2O$  flows.

Table 4. Ohmic resistance ( $R_o$ ) and polarization resistance ( $R_p$ ) data for the cell at high  $H_2$ -3% $H_2O$  flow and  $H_2$ -50% $H_2O$  flow.



## FIGURE CAPTIONS

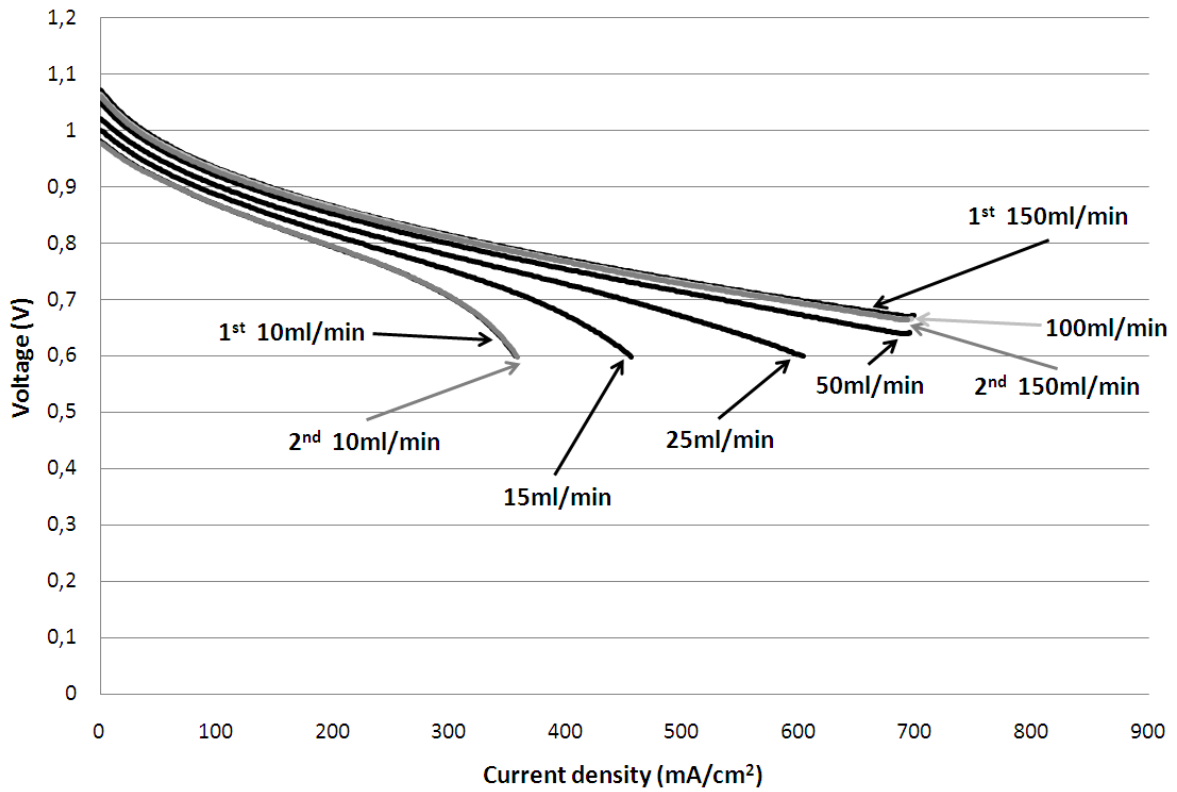


Fig1. I-V performance of a tubular metal-supported cell tested under different H<sub>2</sub> flows.

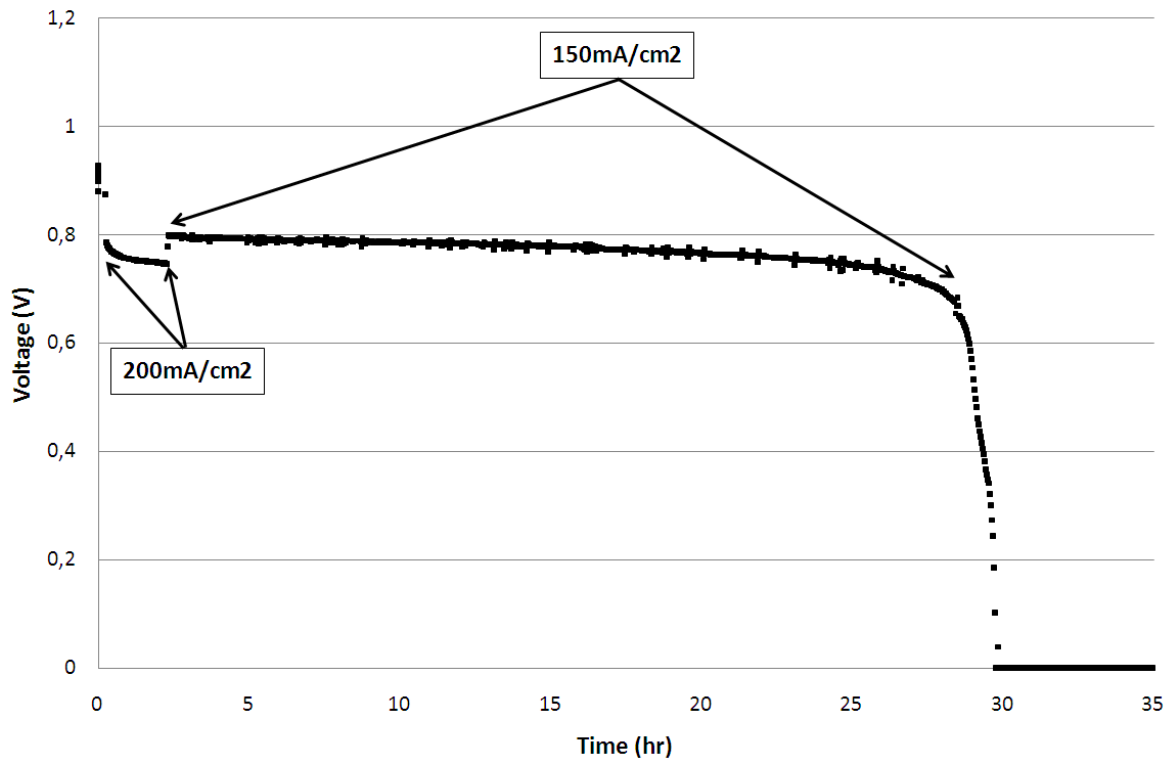


Fig2. Degradation curves for a tubular metal-supported SOFC tested at 800°C under high FU.

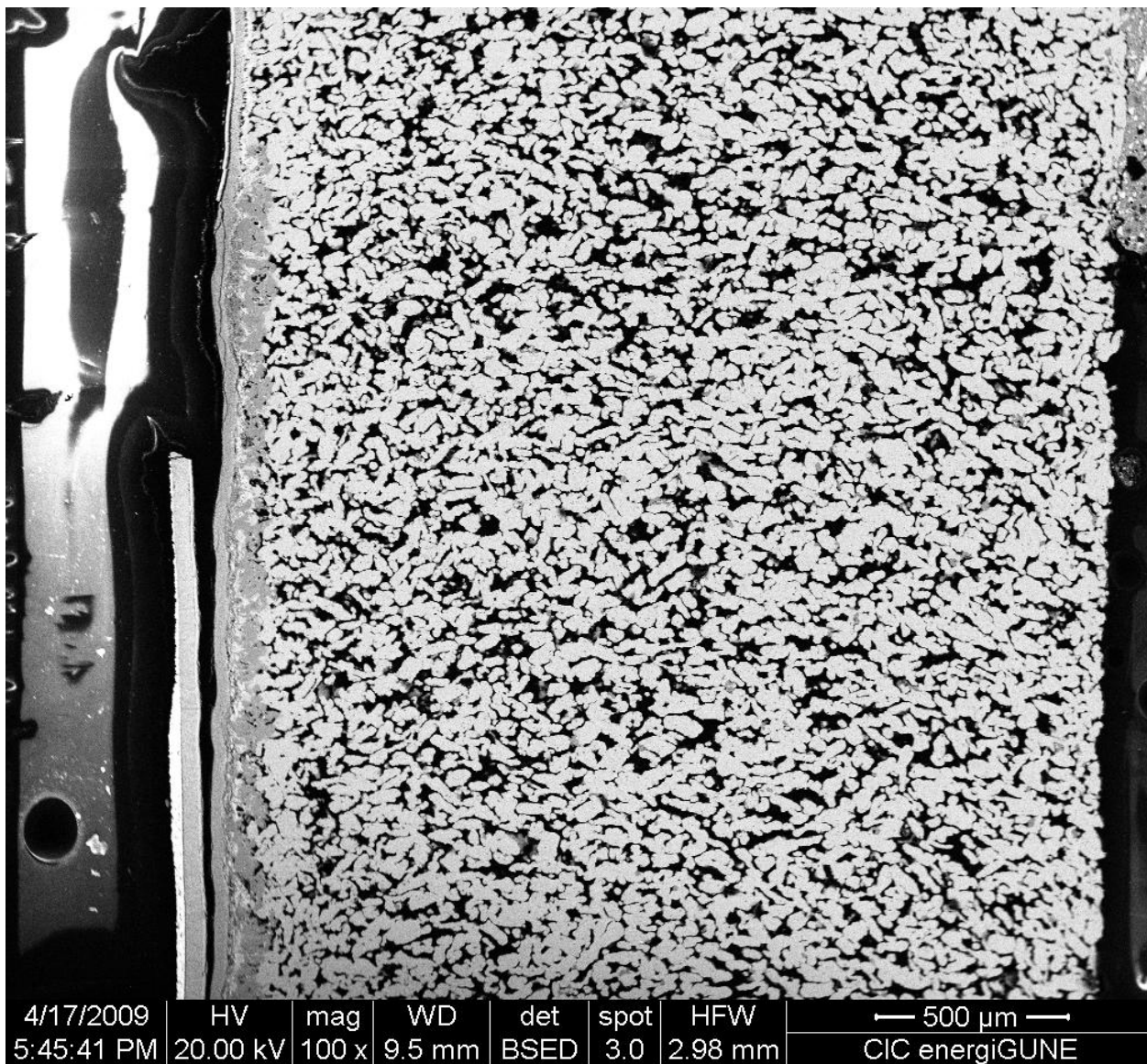


Fig3. SEM image of a cross section of the cell working at 800°C at high FU.

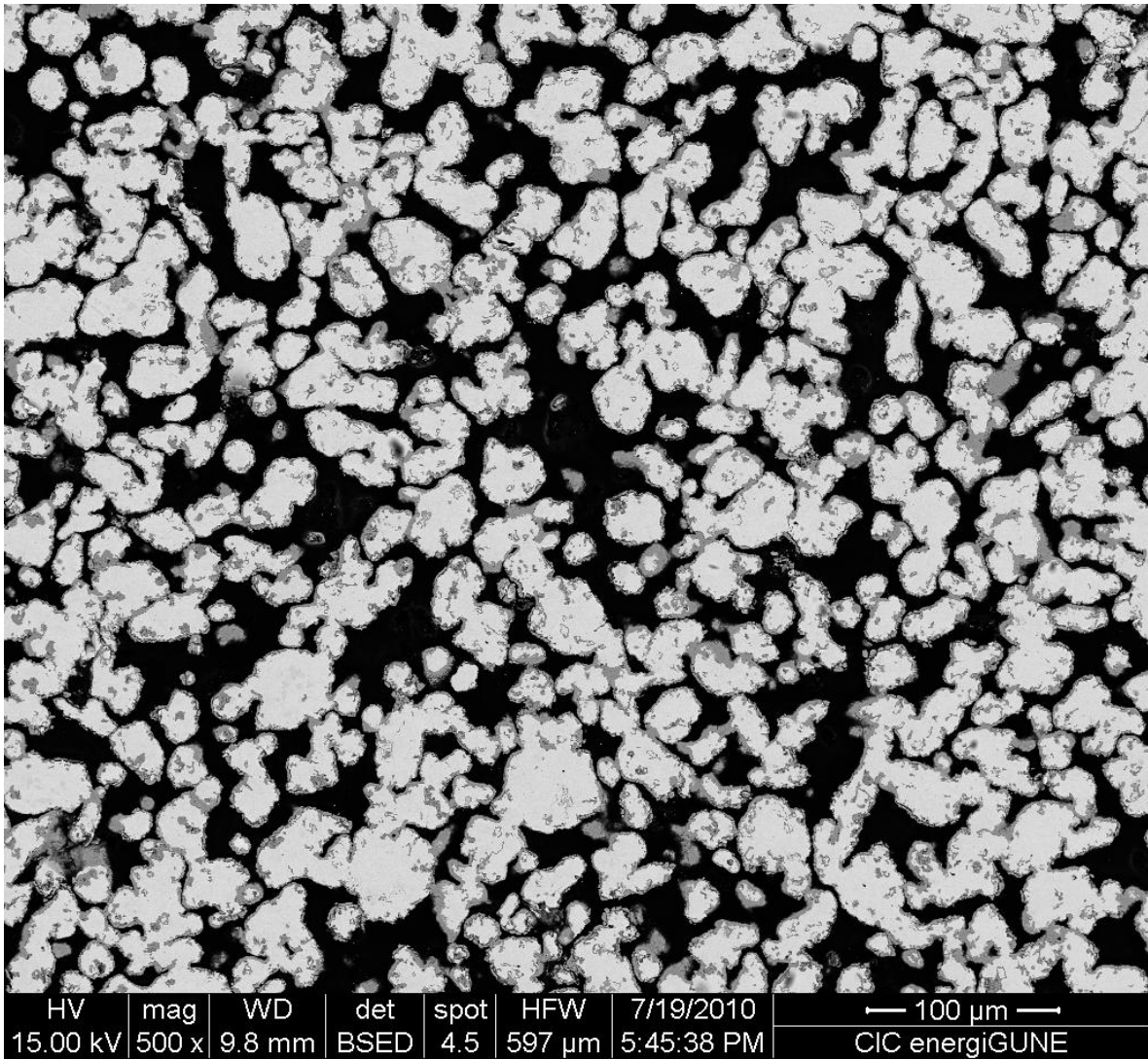


Fig4. SEM image of a cross section of the porous sample oxidized at 850°C in H<sub>2</sub>-50%H<sub>2</sub>O.

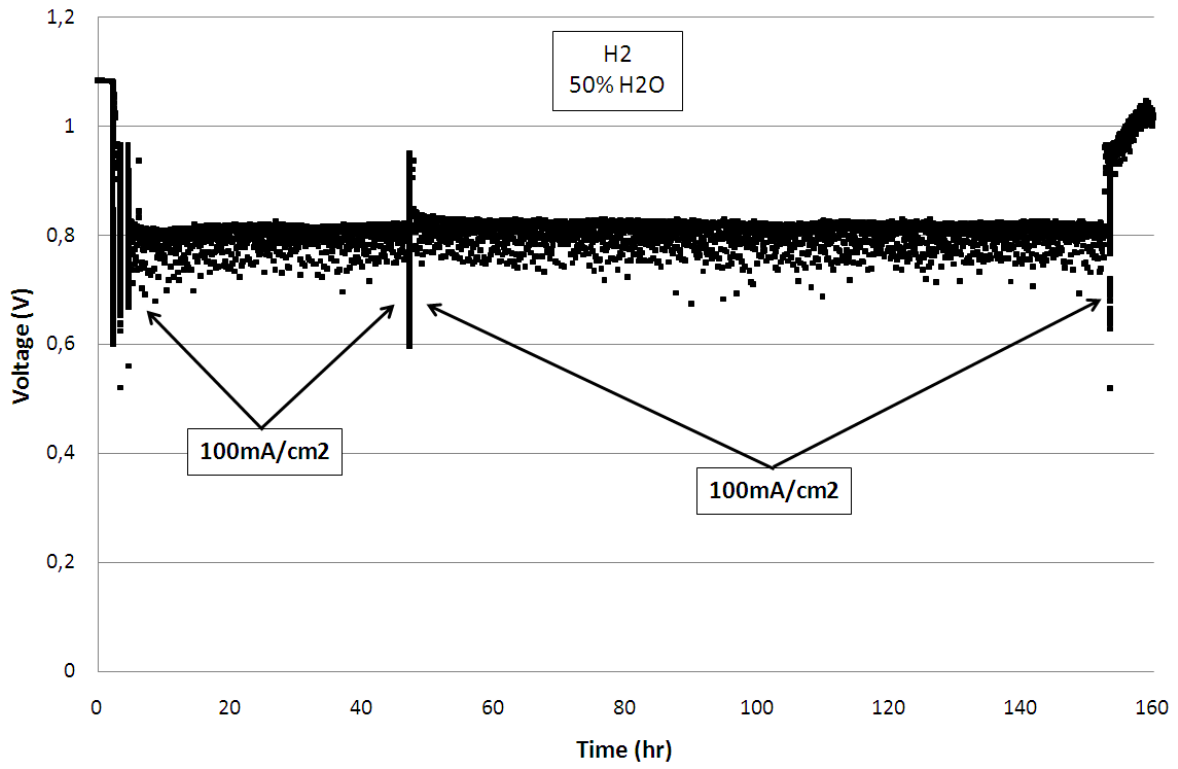


Fig5. Voltage curve for a tubular metal-supported SOFC tested at 800°C in H<sub>2</sub>-50%H<sub>2</sub>O at a constant current density of 100 mA/cm<sup>2</sup>.

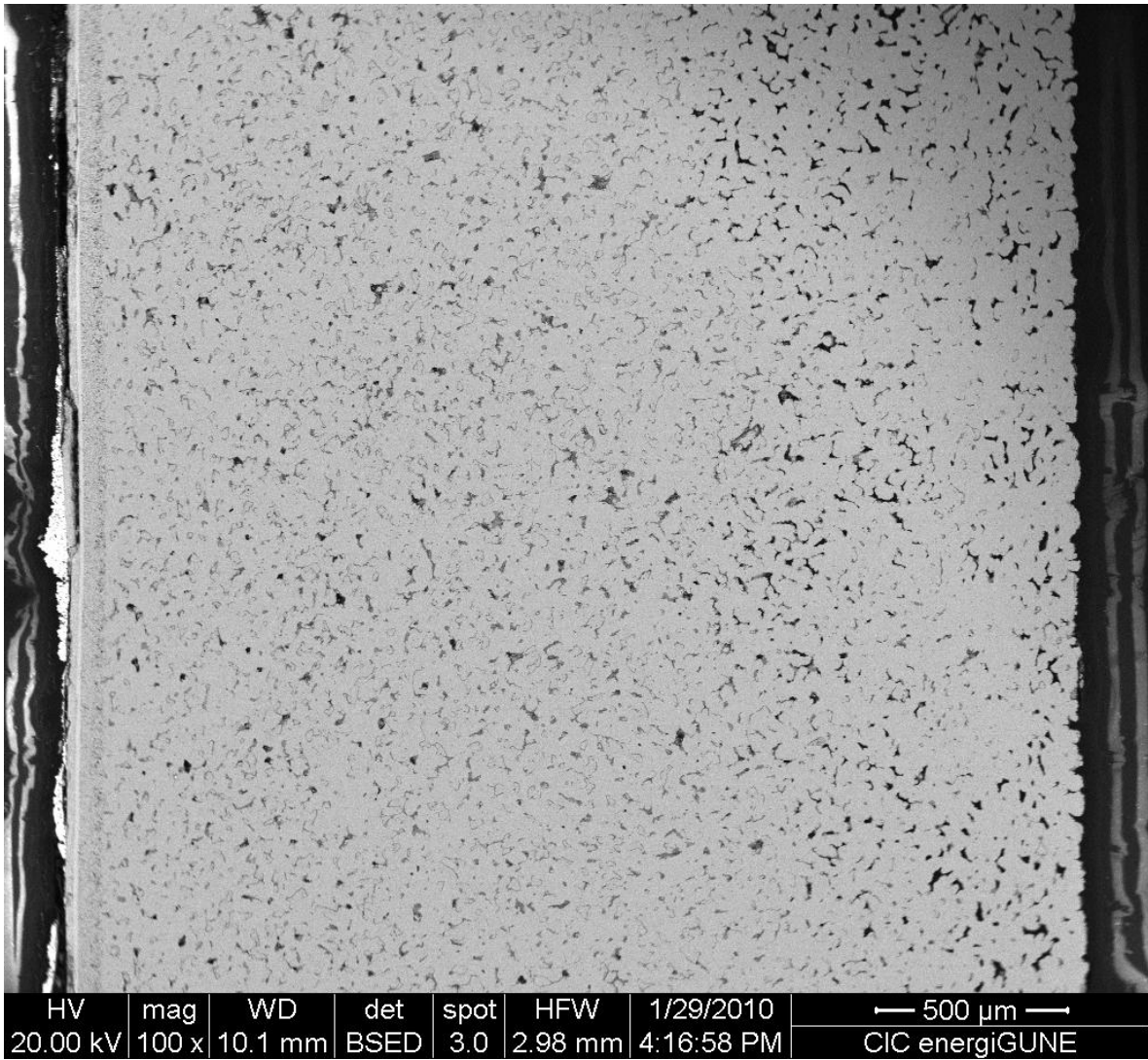
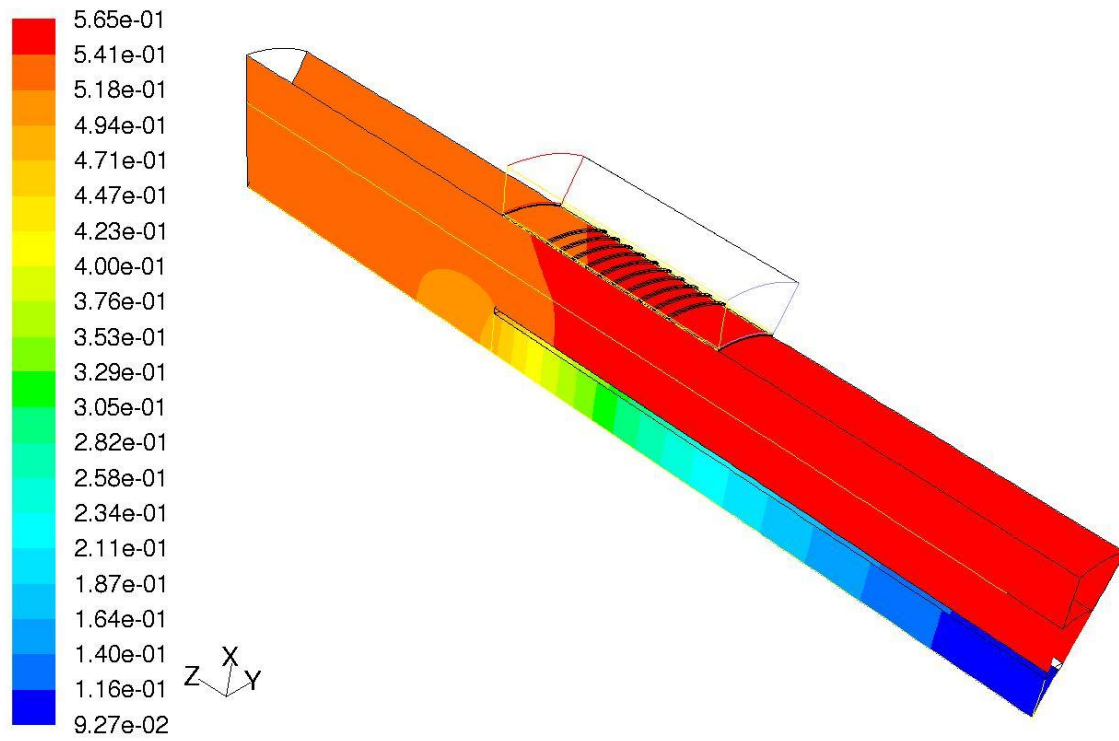
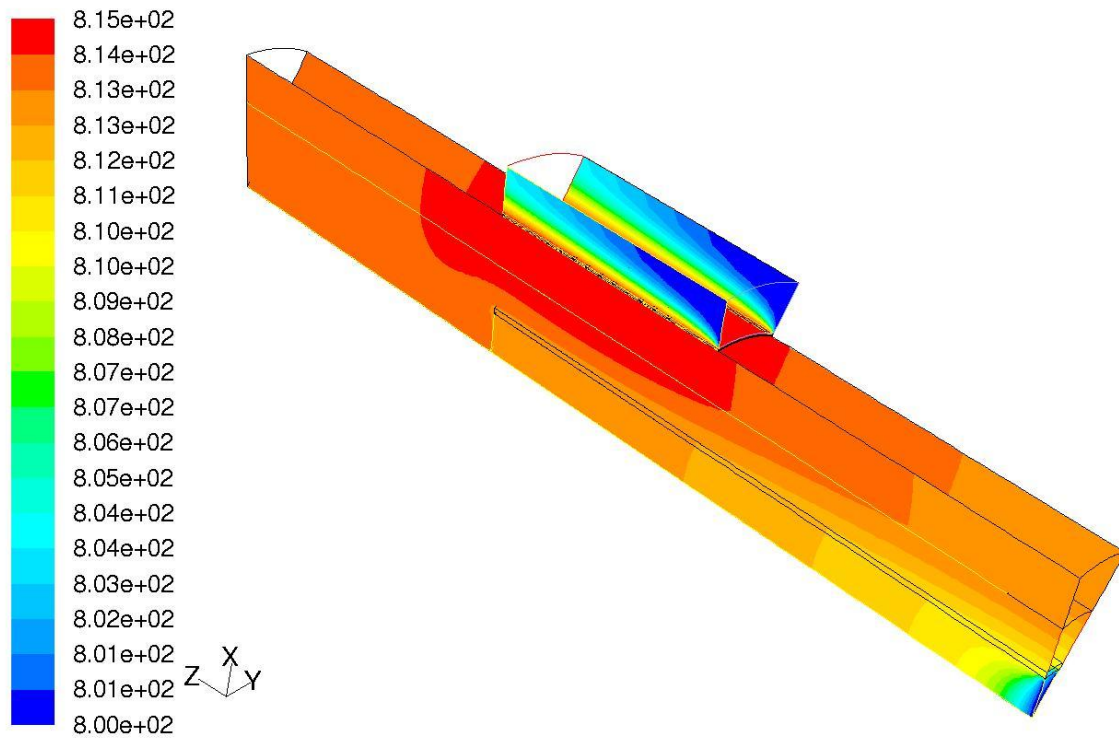


Fig6. SEM image of a cross section of the cell working at 800°C in H<sub>2</sub>-50%H<sub>2</sub>O.



Celda de 4 cm<sup>2</sup>, 200 mA/cm<sup>2</sup>, 800 °C, fuel 97% H<sub>2</sub> / 3% H<sub>2</sub>O  
 Contours of Mole fraction of h<sub>2</sub>o  
 Nov 27, 2009  
 FLUENT 6.3 (3d, dp, pbns, spe, lam)

Fig7. FLUENT model of a cell, oven temperature 800°C and fuel H<sub>2</sub>-3%H<sub>2</sub>O.  
 Contours of mole fraction of H<sub>2</sub>O.



Celda de 4 cm<sup>2</sup>, 200 mA/cm<sup>2</sup>, 800 °C, fuel 97% H<sub>2</sub> / 3% H<sub>2</sub>O  
 Contours of temperatura-c

Nov 27, 2009  
 FLUENT 6.3 (3d, dp, pbns, spe, lam)

Fig8. FLUENT model of a cell, oven temperature 800°C and fuel H<sub>2</sub>-3%H<sub>2</sub>O.  
 Contours of temperature.

## TABLES

Layer	Crofer22APU Support	Anode	Cathode	Pt paste
Conductivity, S/m	870000	8	8700	714300

Table 1. Summary of properties for the porous layers.



Fuel composition (H <sub>2</sub> /H <sub>2</sub> O) volume basis	Total current (A)	Fuel mass flow (kg/s)	Air mass flow (kg/s)
97/03	0.063	1.445·10 <sup>-9</sup>	2.129·10 <sup>-6</sup>

Table 2. Data for the portion modelled. For the whole cell, multiply the figures by 6.

Ro (Ωcm <sup>2</sup> )	Rp (Ωcm <sup>2</sup> )	
	High H <sub>2</sub> -3%H <sub>2</sub> O flow	Low H <sub>2</sub> -3%H <sub>2</sub> O flow
0.21	0.16	0.27

Table 3 Ohmic resistance (Ro) and polarization resistance (Rp) for the cell at high and low H<sub>2</sub>-3%H<sub>2</sub>O flows.

Ro (Ωcm <sup>2</sup> )	Rp (Ωcm <sup>2</sup> )	
	High H <sub>2</sub> -3%H <sub>2</sub> O flow	High H <sub>2</sub> -50%H <sub>2</sub> O flow
0.4 - 0.56	0.26	0.33

Table 4 Ohmic resistance (Ro) and polarization resistance (Rp) for the cell at high H<sub>2</sub>-3%H<sub>2</sub>O flow and H<sub>2</sub>-50%H<sub>2</sub>O flow.